

Absolute negative mobility and current reversals of a meandering Brownian particle

Ralf Eichhorn, Peter Reimann, Peter Hänggi

Angaben zur Veröffentlichung / Publication details:

Eichhorn, Ralf, Peter Reimann, and Peter Hänggi. 2003. "Absolute negative mobility and current reversals of a meandering Brownian particle." *Physica A: Statistical Mechanics and its Applications* 325 (1-2): 101–9. [https://doi.org/10.1016/S0378-4371\(03\)00188-2](https://doi.org/10.1016/S0378-4371(03)00188-2).

Absolute negative mobility and current reversals of a meandering Brownian particle

Ralf Eichhorn^a, Peter Reimann^{a,*}, Peter Hänggi^b

^a*Fakultät für Physik, Universität Bielefeld, Universitätsstraße 25, D-33615 Bielefeld, Germany*

^b*Universität Augsburg, Institut für Physik, Theoretische Physik I, Universitätsstr. 1,
D-86135 Augsburg, Germany*

1. Introduction

To most people it appears obvious that a system at rest, when perturbed by an external static force, responds by moving into the direction of that force. Indeed, if the unperturbed system is at thermal equilibrium then any other kind of behavior, e.g. a permanent motion *without* external force or in the direction *opposite* to the applied force, is forbidden by the second law of thermodynamics, since it could be exploited to

* Corresponding author. Tel.: +41-521-106-6206; fax: +41-521-106-6455.
E-mail address: preimann@physik.uni-bielefeld.de (P. Reimann).

construct a *perpetuum mobile* of the second kind.¹ Far away from thermal equilibrium, however, no basic principles a priori rule out such counter-intuitive effects. In fact, the former case is well-known as *ratchet effect* in non-equilibrium systems possessing an intrinsic asymmetry [2–8], whereas the latter case is known as *absolute negative mobility* (ANM). More precisely, ANM is defined as follows: Upon application of an external static “load” force F of whatever direction the system responds with an average motion (or “current”) which always runs into the direction *opposite* to that of F (provided F is not too large in modulus). Especially, no average current arises when $F = 0$. In other words, the current–load characteristics of the system exhibits a passage through the origin with a negative slope as its most prominent feature. ANM has been investigated in different *quantum mechanical* non-equilibrium systems [9–19], in models of *interacting* Brownian particles [20–25], and, more recently, has also been shown to exist in *classical, single-particle* systems [26–28].

In Ref. [27], several distinct models of the latter class have been shown to exhibit ANM under *slow* non-equilibrium perturbations. In the present paper, we will extend our studies of one of those models from Ref. [27] to the case when it is disequibrated by *moderately fast* perturbations. As it turns out, this system reveals several particularly interesting, new properties, caused by the fact that here two different, new physical mechanisms are governing the occurrence (or not) of ANM. Due to their competing character, the current–load characteristics can be tailored to exhibit additional, qualitatively distinct features, such as multiple current reversals superimposed to ANM (see Fig. 3b).

2. Model

We consider the following two-dimensional overdamped coupled Brownian motion

$$\eta\dot{x}(t) = -\partial_x V(x(t), y(t)) + \sqrt{2\eta k_B T} \xi_x(t), \quad (1)$$

$$\eta\dot{y}(t) = -\partial_y V(x(t), y(t)) + \sqrt{2\eta k_B T} \xi_y(t) + F_{\text{tot}}(t), \quad (2)$$

where k_B is Boltzmann’s constant and η the viscous friction coefficient. As usual, $\xi_x(t)$ and $\xi_y(t)$ denote independent, unbiased, δ -correlated Gaussian noise sources representing the fluctuations due to the thermal environment at temperature T . Furthermore, the Brownian motion is confined to a corridor-like, spatially periodic and symmetric hard-wall potential $V(x, y)$ as depicted in Fig. 1a. Finally, the thermal equilibrium is broken by an externally applied force $F_{\text{tot}}(t)$ composed of a static part F and some unbiased, time-dependent part which will be specified in more detail below (see

¹An apparent counter example [1] is a bubble in a liquid under the action of a force generated by gravitation: it always moves in the direction opposite to the applied force (gravitation), while the force-free setup (in the absence of gravitation) is at thermal equilibrium. However, in this case the (gravitational) force does *not* act on the bubble (system) itself, it only affects the liquid (environment) by giving the buoyancy. Accordingly, no work can be gained and no perpetuum mobile constructed.

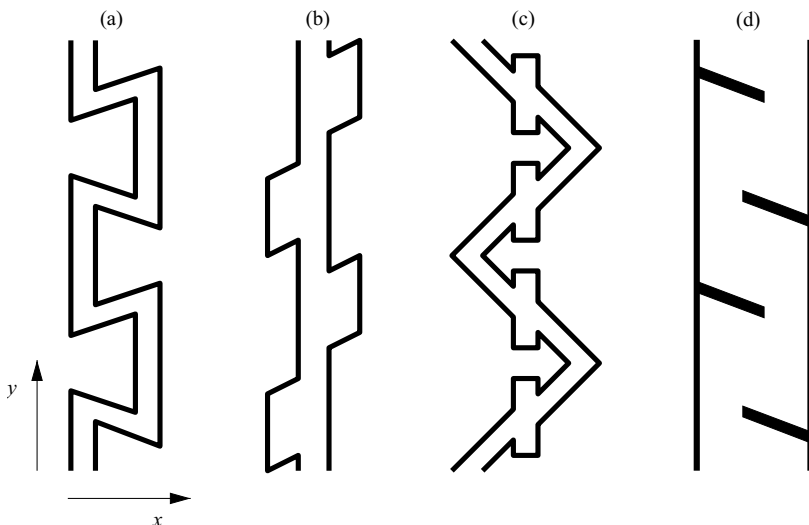


Fig. 1. Different possible geometries of potential landscapes $V(x, y)$ in (1) and (2) that can exhibit ANM. In each case, the particle is confined to the inner white regions where $V(x, y) \equiv 0$; the black walls are defined to have infinite potential. All these hard-wall “corridors” are periodic (shown are two periods) and symmetric under inversion of the y -axis. The common feature of all the different potentials is the existence of particle traps with increasing “stickiness” as the external force strength along the y -axis increases (see main text). (a) The particle is trapped in the corners where the “vertical parts” of the corridor are joined to the “diagonal parts”. Note that the angle enclosed by the “vertical” and diagonal elements is smaller than $\pi/2$. (b) The traps are represented by the attached “fins” and are entered by lateral diffusion along the x -direction while “falling down” the central “backbone”. (c) The vertical parts of the corridor act as traps. The particle “falls into” them when “sliding down the diagonal ramps”. (d) The particle traps are given by the sharp corners between the “corridor walls” and the obstacles.

Eq. (4)). Aiming at mobility properties of this model, our basic quantity of interest is the average particle current

$$\langle \dot{y} \rangle := \lim_{t \rightarrow \infty} \frac{y(t)}{t} \quad (3)$$

along the direction of the externally applied static force F .

The considered hard-wall potential (Fig. 1a) is composed of “vertical parts” (parallel to the y -direction) and intermediate “diagonal parts”, forming a periodic and spatially symmetric “zigzag” pattern. The sharp corners between “vertical” and “diagonal elements”, in combination with the external force, play a key role for the Brownian motion (1), (2) as *particle traps*: Under the action of a purely static force $F_{\text{tot}}(t) \equiv F = \text{const.}$ (which we may assume to be positive due to symmetry reasons), the induced drift of the particle along the y -direction will quickly get stuck in such a corner. An escape out of the corner is then possible only due to the ambient thermal noise when the particle diffusively moves “up” the adjacent diagonal part of the “corridor” against the force F until it reaches the next “vertical element”. The particle thus lingers the longer in this

trap the larger the force F is.² As shown in Refs. [26,27], the existence of such traps with increasing “depth” or “stickiness” as the external force increases can be exploited to generate ANM under sufficiently slow non-equilibrium perturbations $F_{\text{tot}}(t)$.

More generally, the common feature of all the different corridor shapes depicted in Fig. 1 is that each of them provides traps with the above-mentioned “stickiness” property and, thus, can exhibit ANM according to the same basic slow-driving mechanism [27].

The ANM-phenomenon in such corridors is, however, not restricted to adiabatically slow non-equilibrium perturbations [26,27], but may show up for (moderately) fast driving as well. In this latter regime, however, the physical mechanisms for ANM depend on the geometrical details of the “corridor”. The potential landscape from Fig. 1a reveals a particularly rich dynamical behavior in this context as we will discuss in detail in the following.

3. ANM and beyond in the zigzag corridor

We consider a deterministic non-equilibrium perturbation that switches periodically³ between the two states $\pm A$ *moderately fast*, that is, with a sojourn time τ much smaller than the mean escape time out of the traps, but large enough that the particle can at least travel completely through a vertical part of the “corridor” by free drift. Together with the static bias F , the total force $F_{\text{tot}}(t)$ then adopts alternately the values $F \pm A$ within a period 2τ , that means

$$F_{\text{tot}}(t) = F + A \text{sign}[\sin(t\pi/\tau)]. \quad (4)$$

We assume that $F \geq 0$, $A > 0$ and $A > F$, such that the two total forcing states $F + A > 0$ and $F - A < 0$ have opposite sign. As a consequence, a particle that becomes trapped in a corner of the “corridor” from Fig. 1a is typically locked for a short time only, namely until the external force $F_{\text{tot}}(t)$ switches from its current state, e.g. $F + A > 0$, to $F - A < 0$, or vice versa. Correspondingly, thermally induced escapes out of the traps can be neglected. To understand what happens instead, let us consider a particle that is trapped, say, in corner 1 of Fig. 2a by $F_{\text{tot}}(t) = F + A > 0$. After the reversal of $F_{\text{tot}}(t)$ to the state $F - A < 0$ the particle either “falls down vertically” through the “corridor” to the opposite corner 2 (to be trapped again), or else it “slides down the adjacent diagonal branch” and reaches the next “vertical segment” ending up in corner 3, see Fig. 2a. After the next switch of $F_{\text{tot}}(t)$ back to $F + A > 0$, the particle has again these two possibilities to leave its corner, namely “vertically” or “diagonally” (see Fig. 2a). The latter alternative is realized whenever the particle

² The escape process out of the trapping corner can be approximately described [27] as thermally activated surmounting of a potential barrier [29], where the height of the barrier increases linearly with the external force.

³ For the sake of simplicity, we restrict ourselves to the case of a *periodic* non-equilibrium driving. The ANM-phenomenon is expected to be robust against various modifications of this simple choice [26,27].

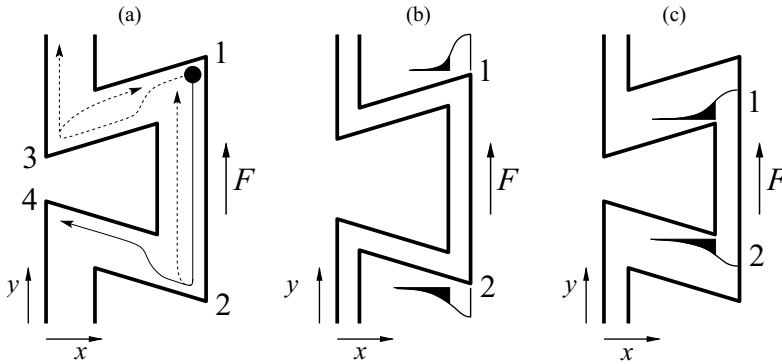


Fig. 2. (a) Typical traveling routes of a particle starting in corner 1 with $F_{\text{tot}}(t) = F - A < 0$, see main text. ANM results from the sketched solid path, whereas the dashed ones do not contribute to ANM. Whenever being “freed” from its trapped state in a corner by a switch of $F_{\text{tot}}(t)$, the particle can either follow the adjacent “vertical branch” or else the “diagonal branch”. The respective probabilities for these two alternatives are determined by the mechanisms illustrated in the panels (b) and (c). (b) When a particle is trapped in a corner its position within this trap can be described according to some probability distribution (due to the ambient thermal noise). This distribution is sketched for $F_{\text{tot}}(t) = F + A > 0$ (corner 1) and for $F_{\text{tot}}(t) = F - A < 0$ (corner 2); note that $F + A > |F - A|$. The filled parts of the sketched distributions represent the probabilities for entering the diagonal branch. (c) If the “corridor” width is small [as in (b)], the “branching probability” is practically not affected by diffusion in x -direction during the “free fall” along the y -direction which follows the reversal of $F_{\text{tot}}(t)$; for wider “corridors” (in particular for wider “diagonal elements”) this mechanism becomes crucial. Sketched are the probability distributions of the particle, after it has passed the width of the diagonal branches in y -direction: “branch” 1 for the large (in modulus) trapping force $F + A > 0$, branch 2 for the small (in modulus) trapping force $F - A < 0$. Again, the filled parts of the distributions indicate the probabilities for entering the diagonal branch.

diffusively overcomes a lateral distance just larger than the width of the vertical parts of Fig. 1a during the (short) time it is locked in a corner and, thus, is located somewhere inside the “diagonal branch” at the reversal of $F_{\text{tot}}(t)$. Exactly, as for a genuine escape out of the trap, this “incomplete escape” process occurs with *greater* probability for *smaller* trapping forces, i.e., the particle “branches off” into the diagonal part more frequently in those corners where it becomes trapped by the smaller force (in modulus) $F - A$ (Fig. 2b). Consequently, it gradually “climbs up the corridor” into the direction *opposite* to the static force F and hence exhibits ANM. This mechanism is more efficient for narrower corridors; then the lateral distance to be overcome for entering a “diagonal branch” is decreased. These predictions are fully confirmed by the simulations of (1), (2), see Fig. 3a.

The above-mentioned force-dependent “branching probability” is modified by an additional mechanism: If the particle falls down vertically along the y -axis just after a reversal of $F_{\text{tot}}(t)$, it can thermally diffuse along the x -direction and subsequently move into the diagonal branch, as long as the “free fall” has not yet covered the width of this diagonal branch. The probability of such a “diffusive branching” process increases with increasing available time for diffusion and, therefore, is *greater* if the particle has been trapped by the *larger* force (in modulus) $F + A$ (the free fall then results from

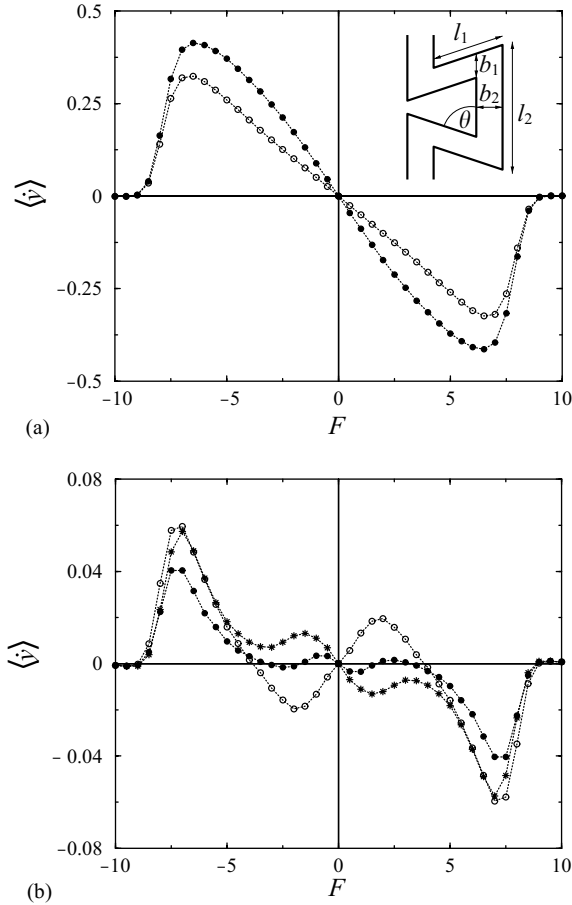


Fig. 3. Current-load characteristics of (1) and (2) for the “zigzag potential” $V(x, y)$ shown in the inset of panel (a). The results are obtained by numerical simulations of (1) and (2). Dimensionless parameters: $l_1 = 1.5$, $\theta = 80^\circ$, $k_B T = 0.1$, $\eta = 1.0$; l_2 is chosen such that the length of the period along the y -axis is identical for all shown cases. (a) Periodic non-equilibrium driving from (4) with $\tau = 1.0$, $A = 10$. Open circles: $b_1 = b_2 = 0.10$, $l_2 = 2.10$. Filled circles: $b_1 = b_2 = 0.01$, $l_2 = 2.01$. (b) Periodic non-equilibrium driving from (5) with $\tau = 1.5$, $\varepsilon = \frac{1}{3}$, $A = 10$. Open circles: $b_1 = b_2 = 0.3$, $l_2 = 2.3$. Filled circles: $b_1 = b_2 = 0.6$, $l_2 = 2.6$. Stars: $b_1 = 1.0$, $b_2 = 0.6$, $l_2 = 3.0$. The interconnecting dotted lines serve as a guide for the eyes.

the *smaller* force $F - A$), see Fig. 2c. Correspondingly, diffusive branching is more efficient for wider corridors, in particular for wider “diagonal segments”. In other words, this physical mechanism works just opposite to the previously discussed “incomplete escape” process and thus weakens or even completely suppresses ANM.

When slightly modifying the so far considered periodic non-equilibrium forcing (4), however, the above-described diffusive branching mechanism can be exploited to generate ANM as well: Between the original states $F \pm A$ of the driving $F_{\text{tot}}(t)$ we insert “breaks” [30] where only the static force F acts along the y -direction, i.e., where

$F_{\text{tot}}(t) \equiv F$ in (2). The duration of these breaks is chosen to cover the fraction $0 \leq \varepsilon < 1$ of each half-period τ , i.e.,

$$F_{\text{tot}}(t) = \begin{cases} F & \text{for } 0 \leq t \bmod \tau < \varepsilon \tau, \\ F + A \text{ sign}[\sin(t\pi/\tau)] & \text{for } \varepsilon \tau \leq t \bmod \tau < \tau. \end{cases} \quad (5)$$

Then, a particle which is locked in a corner due to the force $F_{\text{tot}}(t) = F - A < 0$ (e.g. in corner 2 or 3 of Fig. 2a) will next be subject to $F > 0$ and thus travel along the y -direction. Vice versa, a particle that is trapped by the force $F + A > 0$ (e.g. in corner 1 or 4 of Fig. 2a) remains trapped by the next forcing state $F > 0$ until $F_{\text{tot}}(t)$ switches to $F - A < 0$. Consequently, for small static forces $F \gtrsim 0$ diffusive branching is the prominent ANM-mechanism, whereas for large forces $F \lesssim A$, incomplete escape processes are at the roots of ANM. Together with our observation that these two mechanisms are supported by distinct widths of the corridor we can control either mechanism by adjusting the geometrical properties of the ‘‘corridor’’, thereby creating qualitatively different current–load characteristics with ANM (examples are depicted in Fig. 3b): (i) The current–load curve as illustrated by the stars in Fig. 3b exhibits a *non-monotonic* ANM-effect. (ii) The filled circles in Fig. 3b show a similar non-monotonic behavior, but now giving rise to several current reversals ‘‘superimposed’’ to ANM: Upon increasing F in modulus (starting from $F = 0$) the current first exhibits ANM, afterwards changes its direction to adopt the same orientation as the load force F , and then, for even *larger* F , reverses once more running again into the direction *opposite* to F . (iii) The current–load curve indicated by the open circles in Fig. 3b does not exhibit ANM in the strict sense as defined above (no negative slope at $F = 0$). Instead, the response of the system to an external load F that is not too large is as usually expected, namely a current in the same direction as the applied force F . Surprisingly enough, *upon further increasing F the current all of a sudden switches its direction and runs opposite to the external load.*

4. Discussion

An amazing consequence of ANM arises when the original homogeneous static force F is replaced by a spatially very slowly varying force field $F(y)$, deriving from a potential $W(y)$, i.e., $F(y) = -W'(y)$. Then, ANM still survives locally, with the consequence of a global motion towards the *maxima* of the potential $W(y)$. In other words, ANM is tantamount to the *stabilization of the unstable states* of the potential $W(y)$ [20].

Similarly, as for the quantum mechanical and collective systems mentioned in the introduction, ANM for a single classical Brownian particle is, so far, mainly of principal interest while sweeping applications, e.g. for practical technological purposes or for elucidating some existing natural phenomena are not yet clearly identifiable. However, some directions which may deserve a more detailed exploration in the future could be the separation of different types of particles or the construction of a ‘‘Brownian switch’’ by exploiting the sensitive dependence of the current–load characteristics on the system parameters as exemplified by Fig. 3b, see also Refs. [28,31,32]. Immediate experimental

implementations of our theoretical concepts should be possible in Coulomb blockade systems [33,34], the vortex dynamics in superconductors [35–38], and by means of colloidal suspensions [39].

Acknowledgements

This work has been supported by the DFG under Sachbeihilfe HA1517/13-4, SFB 613, and the Graduiertenkolleg GRK283.

References

- [1] L. Kish, private communication.
- [2] P. Hänggi, R. Bartussek, in: J. Parisi, S.C. Müller, W. Zimmermann (Eds.), *Nonlinear Physics of Complex Systems*, Lecture Notes in Physics, Vol. 476, Springer, Berlin, 1996, pp. 294–308.
- [3] F. Jülicher, A. Ajdari, J. Prost, *Rev. Mod. Phys.* 69 (1997) 1269.
- [4] R.D. Astumian, *Science* 276 (1997) 917.
- [5] P. Reimann, *Phys. Rep.* 361 (2002) 57.
- [6] P. Reimann, P. Hänggi, *Appl. Phys. A* 75 (2002) 169.
- [7] R.D. Astumian, P. Hänggi, *Phys. Today* 55 (11) (2002) 33.
- [8] H. Linke (Ed.), *Ratchets and Brownian motors: basics, experiments and applications*, special issue, *Appl. Phys. A* 75(2) (2002) 167–352.
- [9] T.Y. Banis, I.V. Parshelyunas, Y.K. Pozhela, *Sov. Phys. Semicond.* 5 (1972) 1727.
- [10] V.V. Pavlovich, E.M. Épshtein, *Sov. Phys. Semicond.* 10 (1976) 1196.
- [11] J. Pozhela, *Plasma and Current Instabilities in Semiconductors*, Pergamon Press, Oxford, 1981.
- [12] T.C.L.G. Sollner, E.R. Brown, W.D. Goodhue, H.Q. Le, in: F. Capasso (Ed.), *Physics of Quantum Electron Devices*, Electronics and Photonics, Springer Series, Vol. 28, Springer, Berlin, 1990, pp. 147–180.
- [13] B.J. Keay, S. Zeuner, S.J. Allen, K.D. Maranowski, A.C. Gossard, U. Bhattacharya, M.J.W. Rodwell, *Phys. Rev. Lett.* 75 (1995) 4102.
- [14] A.A. Ignatov, E. Schomburg, J. Grenzer, K.F. Renk, E.P. Dodin, *Z. Phys. B* 98 (1995) 187.
- [15] Y. Dakhnovskii, H. Metiu, *Phys. Rev. B* 51 (1995) 4193.
- [16] R. Aguado, G. Platero, *Phys. Rev. B* 55 (1997) 12 860.
- [17] L. Hartmann, M. Grifoni, P. Hänggi, *Europhys. Lett.* 38 (1997) 497.
- [18] I.A. Goychuk, E.G. Petrov, V. May, *Phys. Lett. A* 238 (1998) 59.
- [19] E.H. Cannon, F.V. Kusmartsev, K.N. Alekseev, D.K. Campbell, *Phys. Rev. Lett.* 85 (2000) 1302.
- [20] P. Reimann, R. Kawai, C. Van den Broeck, P. Hänggi, *Europhys. Lett.* 45 (1999) 545.
- [21] P. Reimann, C. Van den Broeck, R. Kawai, *Phys. Rev. E* 60 (1999) 6402.
- [22] J. Buceta, J.M. Parrondo, C. Van den Broeck, F.J. de la Rubia, *Phys. Rev. E* 61 (2000) 6287.
- [23] C. Van den Broeck, I. Bena, P. Reimann, J. Lehmann, *Ann. Phys. (Leipzig)* 9 (2000) 713.
- [24] S.E. Mangioni, R.R. Deza, H.S. Wio, *Phys. Rev. E* 63 (2001) 041 115.
- [25] B. Cleuren, C. Van den Broeck, *Europhys. Lett.* 54 (2001) 1.
- [26] R. Eichhorn, P. Reimann, P. Hänggi, *Phys. Rev. Lett.* 88 (2002) 190 601.
- [27] R. Eichhorn, P. Reimann, P. Hänggi, *Phys. Rev. E* 66 (2002) 066 132.
- [28] B. Cleuren, C. Van den Broeck, *Phys. Rev. E* 65 (2002) 030101(R).
- [29] P. Hänggi, P. Talkner, M. Borkovec, *Rev. Mod. Phys.* 62 (1990) 251.
- [30] M. Schreier, P. Reimann, P. Hänggi, E. Pollak, *Europhys. Lett.* 44 (1998) 416.
- [31] G.A. Griess, P. Serwer, *Biopolymers* 29 (1990) 1863.
- [32] C. Desruisseaux, G.W. Slater, T.B.L. Kist, *Biophys. J.* 75 (1998) 1228.
- [33] T. Mii, K. Makoshi, *Jpn. J. Appl. Phys.* 35 (1996) 3706.

- [34] M. Stopa, Phys. Rev. Lett. 88 (2002) 146 802.
- [35] J.F. Wambaugh, C. Reichhardt, C.J. Olson, F. Marchesoni, F. Nori, Phys. Rev. Lett. 83 (1999) 5106.
- [36] C.J. Olson, C. Reichhardt, B. Jankó, F. Nori, Phys. Rev. Lett. 87 (2001) 177 002.
- [37] B.Y. Zhu, F. Marchesoni, F. Nori, Physica C, in press.
- [38] F. Marchesoni, B.Y. Zhu, F. Nori, Physica A 325 (2003) 78–91 [these proceedings].
- [39] C. Bechinger, work in progress.